The QCD equation of state at high temperatures

J. H. Weber[1] in collaboration with
A. Bazavov[1] and P. Petreczky[2]

[1]**Michigan State University, CMSE**
[2]Brookhaven National Lab

36th International Symposium on Lattice Field Theory,
Michigan State University, East Lansing, USA, 07/26/2018

Phys. Rev. D97 (2018) no. 1, 014510

Outline

QCD phase diagram

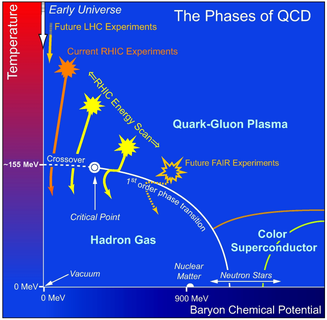

- Asymptotic freedom suggests a weakly-interacting phase[1]
- 2+1 flavor QCD equation of state at zero baryochemical potential has been calculated up to $T \approx 400$ MeV by HotQCD and BW collaborations
- 2+1+1 flavor QCD equation of state at zero baryochemical potential has been calculated up to $T \approx 1$ GeV

[1] Collins, Perry (1975), Cabbibo, Parisi (1975)

QCD phase diagram

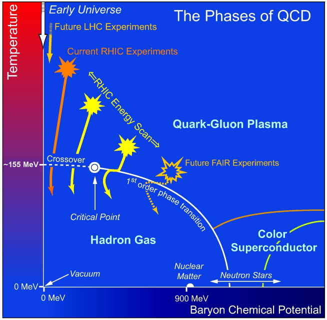

- Asymptotic freedom suggests a weakly-interacting phase[1]
- 2+1 flavor QCD equation of state at zero baryochemical potential has been calculated up to $T \approx 400$ MeV by HotQCD and BW collaborations
- 2+1+1 flavor QCD equation of state at zero baryochemical potential has been calculated up to $T \approx 1$ GeV

For which temperatures is the weak-coupling picture appropriate?

[1] Collins, Perry (1975), Cabbibo, Parisi (1975)

Recent results up to $T = 400$ MeV

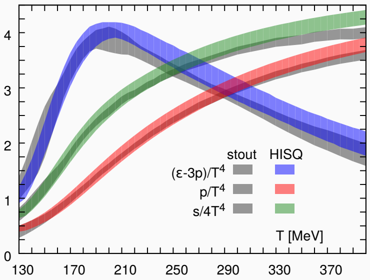

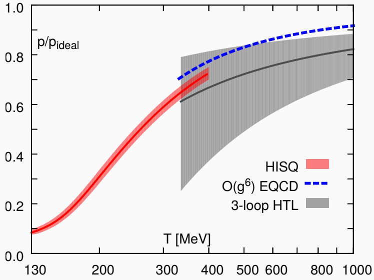

- Comparison of the continuum limit for 2+1 flavors and HISQ[2] and stout[3] actions for the trace anomaly, pressure and entropy density
- The pressure compared with (HTL)[4] and Electrostatic QCD (EQCD)[5] calculations @ NNLO ($\mathcal{O}(g^6)$)

[2] Bazavov et al. [HotQCD] (2014)
[3] Borsanyi et al. [WB] (2014)
[4] Haque et al. (2014)
[5] Laine and Schröder (2006)

Lattice QCD

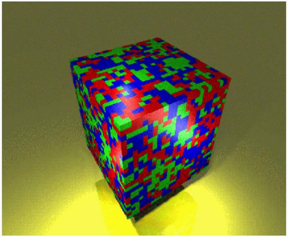

- Switch from Minkowski to Euclidean space – imaginary time formalism
- Define the theory on discrete space-time grid $N_\sigma^3 N_\tau$ with $N_\sigma = 4N_\tau$
- Use (rooted) HISQ[6] action for two light and a physical strange quark
- Use tree-level Symanzik-improved gauge action

- Temperature is set as $T = 1/(aN_\tau)$
- Fix N_τ, dial the lattice spacing to cover a temperature range
- The continuum limit is reached as $1/N_\tau \to 0$
- Discretization errors at fixed T scale as $1/N_\tau^2$ and $1/N_\tau^4$ for HISQ

[6] Follana et al. [HPQCD] (2007)

HISQ data sets

- Previous gauge ensembles (HotQCD)[7]: $m_\pi \approx 160$ MeV

$$
\begin{aligned}
m_\ell &= m_s/20 \\
N_\tau &= 6, 8, 10, 12 \\
\beta &= 5.9, \ldots, 7.825
\end{aligned}
$$

[7] Bazavov et al. [HotQCD] (2014)
[8] Bazavov et al. [TUMQCD] (2018)

HISQ data sets

- Previous gauge ensembles (HotQCD)[7]: $m_\pi \approx 160$ MeV

$$\begin{aligned} m_\ell &= m_s/20 \\ N_\tau &= 6, 8, 10, 12 \\ \beta &= 5.9, \ldots, 7.825 \end{aligned}$$

- Additional gauge ensembles (TUMQCD)[8]: $m_\pi \approx 320$ MeV

$$\begin{aligned} m_\ell &= m_s/5 \\ N_\tau &= 4, 6, 8, 10, 12 \\ \beta &= (7.03, 7.825,)\ 8, 8.2, 8.4 \end{aligned}$$

[7] Bazavov et al. [HotQCD] (2014)
[8] Bazavov et al. [TUMQCD] (2018)

HISQ data sets

- Previous gauge ensembles (HotQCD)[7]: $m_\pi \approx 160$ MeV

$$m_\ell = m_s/20$$
$$N_\tau = 6, 8, 10, 12$$
$$\beta = 5.9, \ldots, 7.825$$

- Additional gauge ensembles (TUMQCD)[8]: $m_\pi \approx 320$ MeV

$$m_\ell = m_s/5$$
$$N_\tau = 4, 6, 8, 10, 12$$
$$\beta = (7.03, 7.825,)\ 8, 8.2, 8.4$$

- What about **quark mass effects** in the combined data set?
- **What about frozen topology on the finest lattices?**

[7] Bazavov et al. [HotQCD] (2014)
[8] Bazavov et al. [TUMQCD] (2018)

Trace anomaly

- The QCD partition function

$$Z = \int DUD\bar{\psi}D\psi \exp\{-S\}, \quad S = S_g + S_f$$

- The pressure is obtained from the trace anomaly via integral method

$$\Theta^{\mu\mu} \equiv \varepsilon - 3p = -\frac{T}{V}\frac{d\ln Z}{d\ln a} \quad \Rightarrow \quad \frac{p}{T^4} - \frac{p_0}{T_0^4} = \int_{T_0}^{T} dT' \frac{\varepsilon - 3p}{T'^5}$$

Trace anomaly

- The QCD partition function

$$Z = \int DUD\bar{\psi}D\psi \exp\{-S\}, \quad S = S_g + S_f$$

- The pressure is obtained from the trace anomaly via integral method

$$\Theta^{\mu\mu} \equiv \varepsilon - 3p = -\frac{T}{V}\frac{d\ln Z}{d\ln a} \quad \Rightarrow \quad \frac{p}{T^4} - \frac{p_0}{T_0^4} = \int_{T_0}^{T} dT' \frac{\varepsilon - 3p}{T'^5}$$

- Subtraction of UV divergences (subtract divergent vacuum contribution evaluated at the same values of the gauge coupling):

$$\begin{aligned} \frac{\varepsilon - 3p}{T^4} &= R_\beta[\langle S_G\rangle_0 - \langle S_G\rangle_T] \\ &- R_\beta R_m[2m_\ell(\langle\bar{\ell}\ell\rangle_0 - \langle\bar{\ell}\ell\rangle_T) + m_s(\langle\bar{s}s\rangle_0 - \langle\bar{s}s\rangle_T)] \end{aligned}$$

$$R_\beta(\beta) = -a\frac{d\beta}{da}, \quad R_m(\beta) = \frac{1}{m}\frac{dm}{d\beta}, \quad \beta = \frac{10}{g^2}$$

Trace anomaly at different quark masses

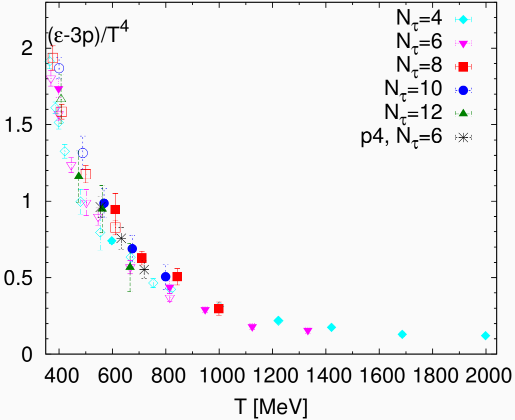

- $\varepsilon - 3p$ with HISQ action for $m_\ell = m_s/20$ or $m_\ell = m_s/5$ at $T > 400 MeV$
- Difference: 10%, 4%, 3% and 1% for $T = 300,\ 400,\ 500$ and 600 MeV
- $\varepsilon - 3p$ with p4 action[9] and $m_\ell = m_s/10$ is consistent for $T > 500$ MeV

[9] Cheng et al. (2008)

Pressure at low temperature

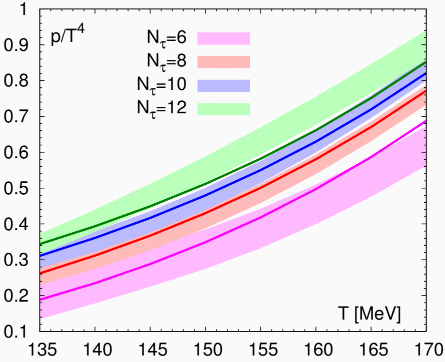

- We have improved the low-temperature region by adding $T = 123$ MeV at $N_\tau = 10$ and $T = 133, 140$ MeV at $N_\tau = 12$[10]
- Bands are interpolations of the lattice data and the lines are Hadron Resonance Gas model results with the cutoff dependent spectrum
- Main origin of these cutoff effects is staggered taste-symmetry violation

[10] Bazavov et al. [TUMQCD] (2016)

Pressure at high temperatures

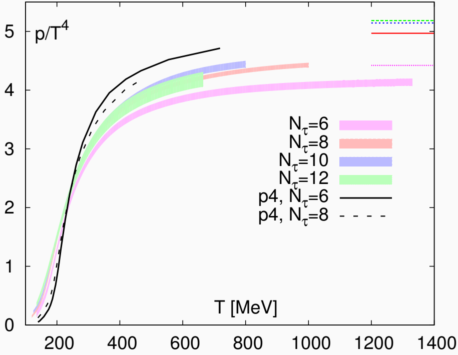

- At high temperatures (i.e. $T > 400$ MeV) the continuum limit is approached with the HISQ or p4 action from below resp. above
- The cutoff dependence of the pressure similar to the one in free theory
- $N_\tau = 12$: large statistical uncertainties, systematics due to $m_\ell = m_s/5$?

Pressure: cutoff dependence

- The cutoff dependence of the **pressure** with HISQ or p4 action is very similar to the cutoff dependence of **quark number susceptibilities**

$$\chi_{2n}^{q} = \frac{\partial^{2n} p(T,\mu_q)}{\partial \mu_q^{2n}},\ n = 1,2,\ q = \ell, s$$

[11] Note: p^q, p^g are NOT directly related to $\Theta_F^{\mu\mu}$, $\Theta_G^{\mu\mu}$: for $m_q = 0 \to p^q > 0$ while $\Theta_F^{\mu\mu} = 0$.

Pressure: cutoff dependence

- The cutoff dependence of the **pressure** with HISQ or p4 action is very similar to the cutoff dependence of **quark number susceptibilities**

$$\chi_{2n}^{q} = \frac{\partial^{2n} p(T, \mu_q)}{\partial \mu_q^{2n}}, \; n = 1, 2, \; q = \ell, s$$

- At high temperatures where the weak-coupling picture is expected to hold we can write the pressure as the sum of the quark and gluon pressures[11] $p(T) = p^q(T) + p^g(T)$

[11] Note: p^q, p^g are NOT directly related to $\Theta_F^{\mu\mu}$, $\Theta_G^{\mu\mu}$: for $m_q = 0 \to p^q > 0$ while $\Theta_F^{\mu\mu} = 0$.

Pressure: cutoff dependence

- The cutoff dependence of the **pressure** with HISQ or p4 action is very similar to the cutoff dependence of **quark number susceptibilities**

$$\chi_{2n}^{q} = \frac{\partial^{2n} p(T, \mu_q)}{\partial \mu_q^{2n}}, \quad n = 1, 2, \quad q = \ell, s$$

- At high temperatures where the weak-coupling picture is expected to hold we can write the pressure as the sum of the quark and gluon pressures[11] $p(T) = p^q(T) + p^g(T)$
- The gluonic pressure is known to have negligible cutoff dependence for improved actions, thus we assume

$$\begin{aligned} p(T) &= p(T, N_\tau) + corr(T, N_\tau) \\ corr(T, N_\tau) &= p^q(T)\left(1 - \frac{p^q(T, N_\tau)}{p^q(T)}\right) \end{aligned}$$

[11] Note: p^q, p^g are NOT directly related to $\Theta_F^{\mu\mu}$, $\Theta_G^{\mu\mu}$: for $m_q = 0 \to p^q > 0$ while $\Theta_F^{\mu\mu} = 0$.

Pressure: correction of cutoff dependence

- We approximate the cutoff dependence of the **quark pressure** by the one of the **second order susceptibilities** χ_2^l [12]

$$\frac{p^q(T, N_\tau)}{p^q(T)} \simeq \frac{\chi_2^l(T, N_\tau)}{\chi_2^l(T)}$$

[12] Calculated in Bazavov et al. (2013)

Pressure: correction of cutoff dependence

- We approximate the cutoff dependence of the **quark pressure** by the one of the **second order susceptibilities** χ_2^l[12]

$$\frac{p^q(T, N_\tau)}{p^q(T)} \simeq \frac{\chi_2^l(T, N_\tau)}{\chi_2^l(T)}$$

- The QCD pressure is below the ideal gas limit by about **15%** at high temperatures $\rightarrow$ we estimate $p_q(T)$ using the ideal quark pressure

[12] Calculated in Bazavov et al. (2013)

Pressure: correction of cutoff dependence

- We approximate the cutoff dependence of the **quark pressure** by the one of the **second order susceptibilities** χ_2^l [12]

$$\frac{p^q(T, N_\tau)}{p^q(T)} \simeq \frac{\chi_2^l(T, N_\tau)}{\chi_2^l(T)}$$

- The QCD pressure is below the ideal gas limit by about **15%** at high temperatures → we estimate $p_q(T)$ using the ideal quark pressure
- The overall estimate of the additive correction

$$corr(T, N_\tau) \simeq p^{q,id-15\%}(T)\left(1 - \frac{\chi_2^l(T, N_\tau)}{\chi_2^l(T)}\right)$$

[12] Calculated in Bazavov et al. (2013)

Pressure: continuum limit

- At **high temperatures** the dominant cutoff dependence of $p(T, N_\tau)$ is like the one of the **ideal quark gas**, thus $p(T, N_\tau) - p(T) \sim 1/N_\tau^4$

[13] We estimate systematic uncertainties from the difference to $1/N_\tau^2$ fit for $T < 400$ MeV

Pressure: continuum limit

- At **high temperatures** the dominant cutoff dependence of $p(T, N_\tau)$ is like the one of the **ideal quark gas**, thus $p(T, N_\tau) - p(T) \sim 1/N_\tau^4$
- At **low temperatures** the dominant cutoff effects are due to staggered **taste-symmetry violations** and scale like $p(T, N_\tau) - p(T) \sim 1/N_\tau^2$

[13] We estimate systematic uncertainties from the difference to $1/N_\tau^2$ fit for $T < 400$ MeV

Pressure: continuum limit

- At **high temperatures** the dominant cutoff dependence of $p(T, N_\tau)$ is like the one of the **ideal quark gas**, thus $p(T, N_\tau) - p(T) \sim 1/N_\tau^4$
- At **low temperatures** the dominant cutoff effects are due to staggered **taste-symmetry violations** and scale like $p(T, N_\tau) - p(T) \sim 1/N_\tau^2$
- We use $1/N_\tau^4$ fit for $T > 200$ MeV and conservative systematic errors[13]

[13] We estimate systematic uncertainties from the difference to $1/N_\tau^2$ fit for $T < 400$ MeV

Pressure: continuum limit

- At **high temperatures** the dominant cutoff dependence of $p(T, N_\tau)$ is like the one of the **ideal quark gas**, thus $p(T, N_\tau) - p(T) \sim 1/N_\tau^4$
- At **low temperatures** the dominant cutoff effects are due to staggered **taste-symmetry violations** and scale like $p(T, N_\tau) - p(T) \sim 1/N_\tau^2$
- We use $1/N_\tau^4$ fit for $T > 200$ MeV and conservative systematic errors[13]
- In 200 MeV $< T < 660$ MeV we have four lattice spacings to perform continuum extrapolations, in 660 MeV $< T < 800$ MeV – three, and for $T > 800$ MeV we can only provide a continuum estimate

[13] We estimate systematic uncertainties from the difference to $1/N_\tau^2$ fit for $T < 400$ MeV

Pressure: correction and continuum

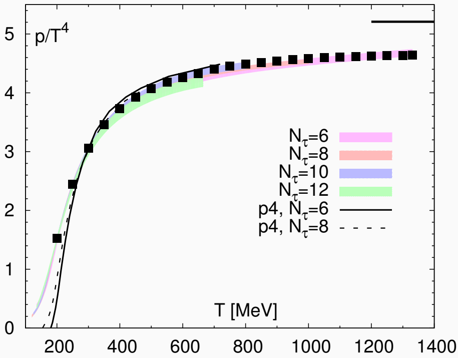

- Corrected pressure at fixed cutoff (HISQ: bands & p4 action: lines) and the explicit continuum limit/estimate (black boxes) all coincide.

Trace anomaly above 800 MeV

- No statistically significant cutoff dependence in the trace anomaly for $N_\tau \geq 8$ and $T > 300$ MeV $\rightarrow$ unsurprising in weak-coupling picture[14]
- Continuum estimate of $\epsilon - 3p$ from a combined interpolation for $N_\tau = 8,\ 10$ and 12 in the interval 300 MeV $< T < 1000$ MeV

[14] Weak coupling suggests cutoff effects of the trace anomaly as $\sim \alpha_s^3 a^2 = \alpha_s^3/(N_\tau T)^2$

[15] Cutoff effects for $N_\tau = 6$ tend to be larger than for $N_\tau = 4$ due to compensating higher order terms, cf. e.g. static quark-antiquark free energies, Bazavov et al. [TUMQCD] (2018)

[16] We tacitly assume a mild T dependence for cutoff effects at $T > 1$ GeV

Trace anomaly above 800 MeV

- No statistically significant cutoff dependence in the trace anomaly for $N_\tau \geq 8$ and $T > 300$ MeV $\rightarrow$ unsurprising in weak-coupling picture[14]
- Continuum estimate of $\epsilon - 3p$ from a combined interpolation for $N_\tau = 8,\ 10$ and 12 in the interval 300 MeV $< T < 1000$ MeV
- The $N_\tau = 4$ and 6 results for $\epsilon - 3p$ lie below this continuum estimate
- We rescale the $N_\tau = 6$ and 4 results for the trace anomaly by factors 1.4 and 1.2, respectively[15], to bring them in agreement with the continuum estimate for 800 MeV $< T < 1000$ MeV[16]

[14] Weak coupling suggests cutoff effects of the trace anomaly as $\sim \alpha_s^3 a^2 = \alpha_s^3/(N_\tau T)^2$

[15] Cutoff effects for $N_\tau = 6$ tend to be larger than for $N_\tau = 4$ due to compensating higher order terms, cf. e.g. static quark-antiquark free energies, Bazavov et al. [TUMQCD] (2018)

[16] We tacitly assume a mild T dependence for cutoff effects at $T > 1$ GeV

Trace anomaly above 800 MeV

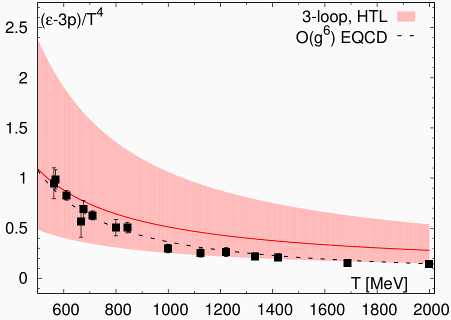

$N_\tau = 6$ and 4 data are rescaled by factors 1.4 and 1.2

Trace anomaly above 800 MeV

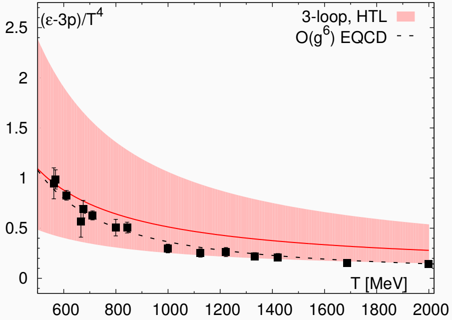

$N_\tau = 6$ and 4 data are rescaled by factors 1.4 and 1.2

- Generous uncertainties of 40% and 20% of rescaled $N_\tau = 6$ and 4 data
- Then perform a spline interpolation of the combined $N_\tau = 12,\ 10,\ 8,\ 6$ and 4 data in the temperature interval 400 MeV $< T <$ 2000 MeV

Trace anomaly above 800 MeV

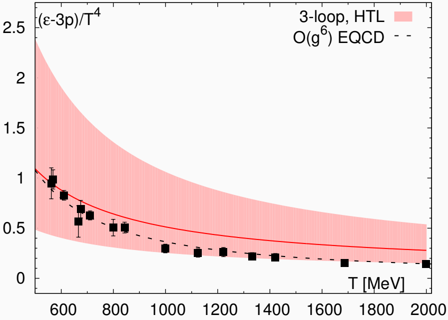

$N_\tau = 6$ and 4 data are rescaled by factors 1.4 and 1.2

- Generous uncertainties of 40% and 20% of rescaled $N_\tau = 6$ and 4 data
- Then perform a spline interpolation of the combined $N_\tau = 12,\ 10,\ 8,\ 6$ and 4 data in the temperature interval 400 MeV $< T < 2000$ MeV
- Integrate the trace anomaly from $T = 660$ MeV to 2000 MeV to get the pressure and the entropy density

Weak-coupling expansions

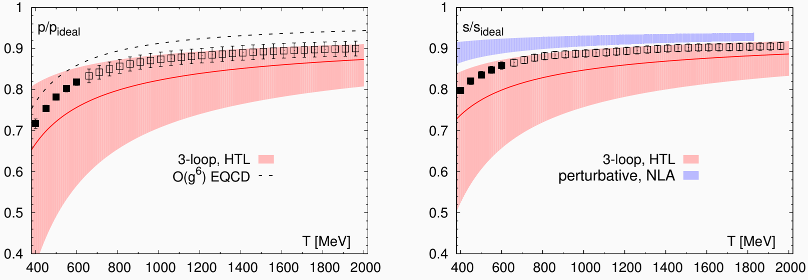

- Uncertainty of continuum estimate has been conservatively doubled to account for possible systematic errors at high temperatures
- Left: Comparison of the pressure obtained on the lattice with the HTL[17] and EQCD[18] results
- Right: Comparison of the entropy density obtained on the lattice with the HTL and NLA[19] results

[17] Haque et al. (2014)
[18] Laine and Schröder (2006)
[19] Rebhan (2003)

Comparison to 2+1+1 flavor QCD

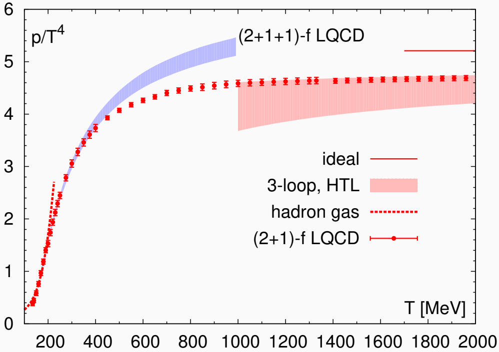

- Considerably smaller errors than the previous HISQ result[20]
- HISQ result at $T = 500$ MeV is 1.5σ higher than stout result[21]
- Only about **3%** lower at $T \approx 400$ MeV than 2+1+1 flavor stout result[22]

[20] Bazavov et al. [HotQCD] (2014)
[21] Borsanyi et al. [WB] (2014)
[22] Borsanyi et al. [WB] (2016)

Weak-coupling results with 2+1 or 2+1+1 massless flavors

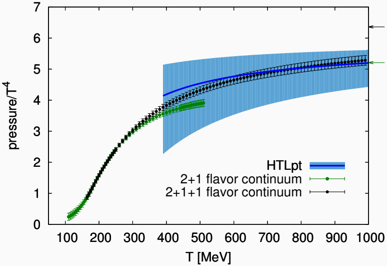

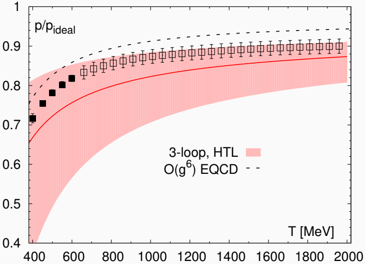

- Left: Comparison of the 2+1+1 flavor pressure obtained with stout action[23] with the 2+1+1 massless flavor HTL result[24]
- Right: Comparison of the 2+1 flavor pressure obtained with HISQ action with the 2+1 massless flavor HTL[25] and EQCD[26] results
- Apparently charm quark mass effects are important for $T \lesssim 1\,\text{GeV}$

[23] Borsanyi et al. [WB] (2016)
[24] Andersen et al. (2010)
[25] Haque et al. (2014)
[26] Laine and Schröder (2006)

Conclusion

- Significantly improved errors compared to previous results by the HotQCD collaboration for the 2+1 flavor QCD equation of state at zero baryochemical potential and extended to higher temperatures
- At temperatures above 400 MeV we use ensembles with $m_\ell = m_s/5$, the quark mass effects are covered within the statistical uncertainties
- Up to 660 MeV we perform the continuum limit with four N_τ
- At high temperatures cutoff effects in the pressure are similar to the those in quark number susceptibilities
- Three different methods to estimate the continuum pressure up to 1330 MeV
- In the interval 660 to 2000 MeV we provide a continuum estimate based on the rescaled $N_\tau = 6$ and 4 results
- Reasonable agreement between the weak-coupling results and the lattice at high temperature

Staggered taste-symmetry violation

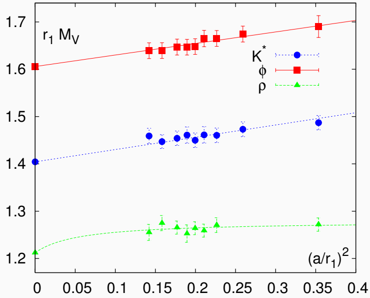

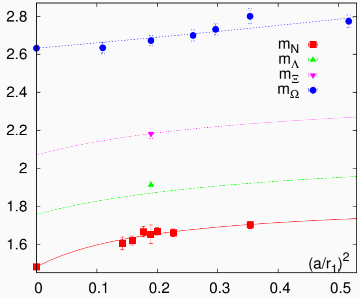

- Distortions and degeneracies for PS mesons with HISQ – well studied
- Smaller distortions for HISQ spectrum of other hadrons
- Include a parametrization of the distortions in hadron resonance gas

$$\ln \mathcal{Z}^H(m_i, T, V) = \mp \frac{Vd_h}{2\pi^2} \int_0^\infty dk k^2 \ln(1 \mp e^{-E_h/T})$$

Distorted HRG

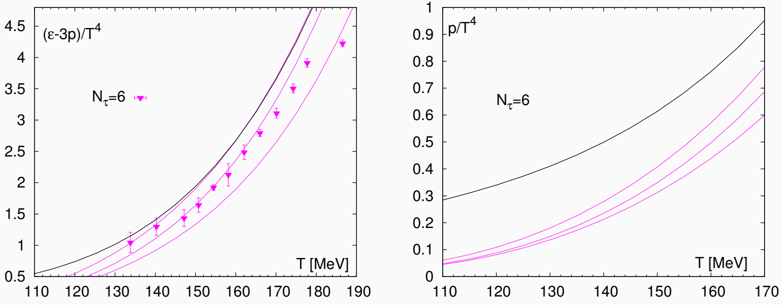

- Lines correspond to undistorted HRG, only distorted PS mesons, only distorted ground states, and HRG with fully distorted spectrum
- Distortion of PS mesons dominant, systematic error from variation
- Larger hadron masses reduce the contribution to the pressure
- Larger mass states contribute more to $\varepsilon - 3p$ → partial compensation

Quark mass dependence

Open symbols: $m_\ell = m_s/20$ – Filled symbols: $m_\ell = m_s/5$

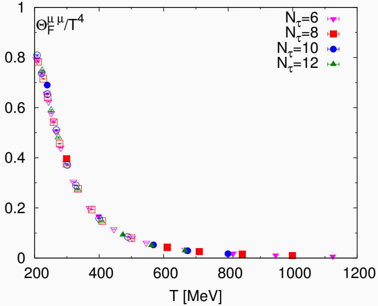

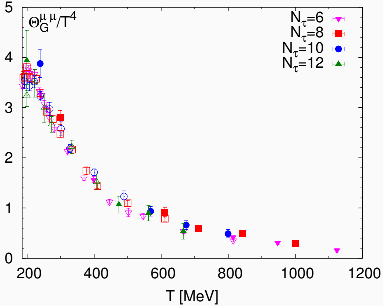

Quark mass dependence

Open symbols: $m_\ell = m_s/20$ – Filled symbols: $m_\ell = m_s/5$

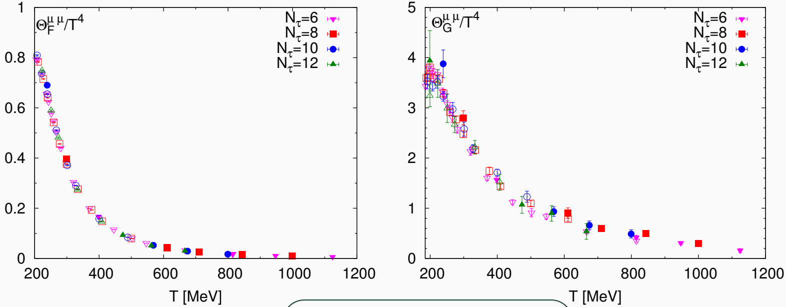

$$R_\beta R_m \, 2m_\ell(\langle\bar{\ell}\ell\rangle_0 - \langle\bar{\ell}\ell\rangle_T)$$

- After adjusting for the **explicit m_ℓ dependence** (i.e. using $m_s/20$ instead of $m_s/5$: the quark contribution $\Theta_F^{\mu\mu}$ is insensitive to m_ℓ
- Cutoff effects, quark mass effects and statistical errors of $\Theta_F^{\mu\mu}$ are tiny

Quark mass dependence

Open symbols: $m_\ell = m_s/20$ – Filled symbols: $m_\ell = m_s/5$

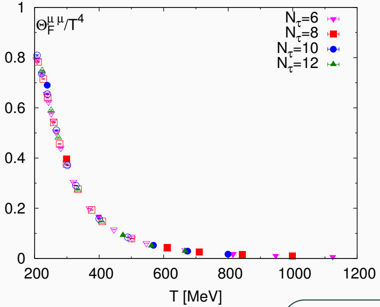

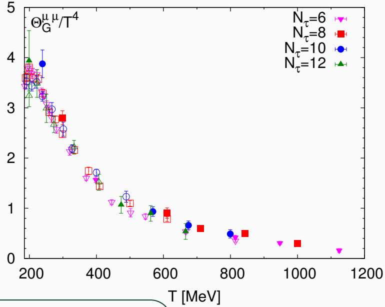

$$R_\beta R_m \, 2m_\ell(\langle\bar{\ell}\ell\rangle_0 - \langle\bar{\ell}\ell\rangle_T)$$

- After adjusting for the **explicit m_ℓ dependence** (i.e. using $m_s/20$ instead of $m_s/5$: the quark contribution $\Theta_F^{\mu\mu}$ is insensitive to m_ℓ
- Cutoff effects, quark mass effects and statistical errors of $\Theta_F^{\mu\mu}$ are tiny
- The gluon contribution $\Theta_G^{\mu\mu}$ depends implicitly on m_ℓ through the sea
- Cutoff effects and quark mass effects of $\Theta_G^{\mu\mu}$ are significant

Slow topological tunneling

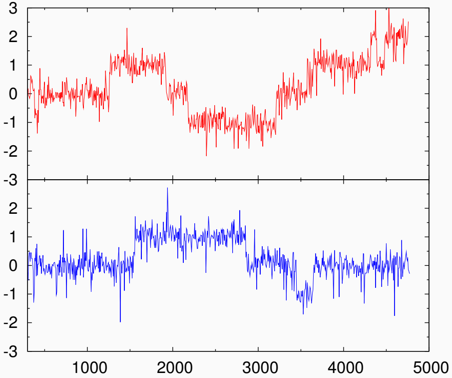

- Two streams of finest HotQCD lattices[27] ($\beta = 7.825$, $m_\ell = m_s/20$)
- Topological tunneling is slow, but still at acceptable rates

[27] Bazavov et al. [HotQCD] (2014)

Frozen topology

β	plaq.	$\langle\bar{\psi}\psi\rangle_\ell$	$\langle\bar{\psi}\psi\rangle_s$	rect.	Q	stream
	0.6641244(21)	0.0026400(66)	0.0117787(51)	0.4607658(29)	2	a
8.0	0.6641256(15)	0.0026061(122)	0.0117719(76)	0.4607666(23)	1	b
	0.6641257(24)	0.0025923(87)	0.0117889(59)	0.4607666(35)	0	c
	0.6738855(16)	0.00207849(52)	0.0095507(55)	0.4744956(24)	2	a
8.2	0.6738854(12)	0.00199916(69)	0.0095271(60)	0.4744943(17)	0	b
	0.6738865(12)	0.00201003(95)	0.0095399(75)	0.4744971(18)	0	c
	0.6830217(14)	0.00171386(47)	0.0078134(48)	0.4874515(22)	2	a
8.4	0.6830200(17)	0.00158675(57)	0.0077629(71)	0.4874514(28)	0	b
	0.6830187(12)	0.00161808(63)	0.0077963(54)	0.4874474(18)	0	c

- Streams with frozen topology in different sectors are generated by hand
- Separate measurement of plaquette, rectangle, light and strange quark condensates at $T = 0$ for different topological sectors $Q = 0,\ 1,\ 2$
- Possibly systematic dependence on topology for light quark condensate
- Topology effects are not statistically relevant for full trace anomaly

Static energy at different quark masses

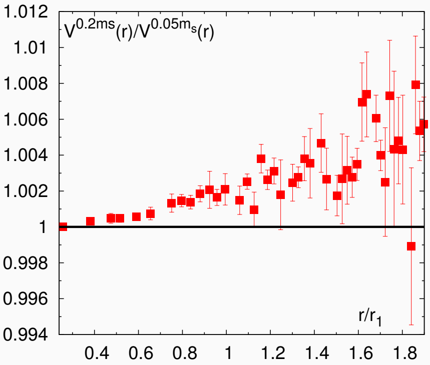

- Ratio of static energy for different quark masses at $\beta = 7.03$
- Increasing with distances, 0.1% (0.2%) deviation at $0.8\,r_1$ (r_1)
- r_1/a resp. (r_2/a) about 1% resp. (0.3%) smaller for $m_\ell = m_s/5$